

# Temporal coarse-graining and elimination of slow dynamics with the generalized Langevin equation for time-filtered observables

Roland R. Netz

*Fachbereich Physik, Freie Universität Berlin, 144195 Berlin, Germany and  
Centre for Condensed Matter Theory, Department of Physics,*

*Indian Institute of Science, Bangalore 560012, India*

(Dated: September 20, 2024)

By exact projection in phase space we derive the generalized Langevin equation (GLE) for time-filtered observables. We employ a general convolution filter that directly acts on arbitrary phase-space observables and can involve low-pass, high-pass, band-pass or band-stop components. The derived filter GLE has the same form and properties as the ordinary GLE but exhibits modified potential, mass and memory friction kernel. Our filter-projection approach has diverse applications and can be used to i) systematically derive temporally coarse-grained models by low-pass filtering, ii) undo data smoothening inherent in any experimental measurement process, iii) decompose data exactly into slow and fast variables that can be analyzed separately and each obey Liouville dynamics. The latter application is suitable for removing slow transient or seasonal (i.e. periodic) components that do not equilibrate over simulation or experimental observation time scales and constitutes an alternative to non-equilibrium approaches. We derive integral formulas for the GLE parameters of filtered data for general systems. For the special case of a Markovian system we derive the filter GLE memory kernel in closed form and show that low-band pass smoothening of data induces exponentially decaying memory.

## I. INTRODUCTION

Doing science often means understanding time-series data or trajectories, which are measurements of observables over time and stem from computer simulations, at varying levels of modeling, or from experiments. When analyzing such trajectories, the problem of time-scale multiplicity arises: In many cases, the process of interest is coupled to microscopic dynamics at much shorter time scales, e.g., observables describing protein-folding dynamics at milliseconds to seconds often include contributions from molecular vibrations on the femtosecond time scale and from water-binding dynamics at the picosecond time scale [1, 2]. In other cases, trajectories are perturbed by processes taking place on much longer times than one is interested in. For example, motility experiments on living cells are influenced by cell-division dynamics [3], daily weather dynamics is coupled to seasonal weather changes [4]. The concept of time-scale separation describes idealized situations where time scales much shorter or longer than the time scale of interest need not be considered since they essentially decouple [5], here we are interested in systems where this decoupling does not take place.

The problem of short and in many applications irrelevant time scales in experimental or simulated trajectories is often simply ignored by recording data at a sufficiently low resolution, so that fast processes are not captured. This approach is unsatisfactory, since it is difficult to construct a model that captures all aspects of the long-time system dynamics from highly discretized data [6]. A more systematic approach to eliminate fast processes is coarse-graining, which allows to build molecular models that do only include a subset of essential microscopic degrees of freedom. An early example are molecular dynam-

ics models that replace electronic degrees of freedom by effective atomistic interaction potentials, current coarse-grained models unite atoms into molecular groups and molecules into supramolecules and are used to describe large-scale protein, RNA and DNA properties [1, 2, 7–11]. By reducing the number of degrees of freedom, the resulting coarse-grained models not only require fewer computations per time step but also eliminate fast dynamics, so that the simulation time step can be increased. The challenge of coarse graining is to define suitable degrees of freedom and to construct their effective interactions, which can be met by machine-learning techniques [12]. However, an essentially unsolved problem is that the coarse-grained dynamic equation of motion becomes non-Markovian, which is relevant for recovering correct long-time dynamics but is difficult to derive and to implement numerically [13, 14]. The filtering-projection approach introduced in this paper can be used to systematically construct temporally coarse-grained models with systematically reduced fast dynamics that accurately preserve the long-time observable dynamics.

The converse problem of long time scales that are present in the system and that couple to the process of interest is even more subtle. It is undisputed that the Hamiltonian of a large enough system, which eventually would encompass the entire universe, becomes autonomous and thus independent of time [15], in which limit the standard time-independent Liouville operator describes the time evolution of the system and in the stationary state (if it exists and is reached on relevant time scales) equilibrium statistical mechanics applies. This changes when the described system is made finite and instead put in contact with a time-varying environment, in which case the Hamiltonian becomes time-dependent. Here one deals with an intrinsically non-equilibrium sit-

uation, i.e. the system is typically far from equilibrium even in its stationary state (if there is one) and the needed theoretical concepts are much less developed than for equilibrium scenarios [16–30]. Also for these situations, our filtering-projection approach can be used to systematically eliminate the long-time transient or oscillatory data components and thus circumvents the need to deal with non-equilibrium effects in the data.

The equation that exactly describes the dynamics of an arbitrary observable over time, for example the position or shape of a molecule, the degree of folding of a protein or the reaction coordinate describing a chemical reaction, is the generalized Langevin equation (GLE) [31, 32], which is an integro-differential equation for a general time-dependent phase-space observable. The GLE is derived from the Hamiltonian for an arbitrarily complex many-body system and generalizes the Newtonian equation of motion by explicitly accounting for the coupling of the observable to its responsive environment in terms of non-Markovian friction and a time-dependent force. Thus, the GLE correctly accounts for the loss of information when projecting the high-dimensional phase-space dynamics onto the low-dimensional observable dynamics and constitutes an exact coarse-graining method. Several methods to extract all GLE parameters from time-series data exist [33–36]. The GLE has been applied to bond-length vibrations, dihedral rotations, chemical reactions in solvents and protein folding [13, 14, 37–40] and also more complex systems, such as the motion of living organisms and financial and meteorological data [15, 41–43]. But the problem of data time-scale multiplicity is also encountered when using the GLE, mostly in the form of numerical convergence problems when extracting the GLE parameters from trajectories.

We here introduce convolution filtering in conjunction with projection as a method to deal with time-scale multiplicity problems in time series data. One central result is that a convolution-filtered trajectory still obeys Liouville dynamics and thus can be treated by exact phase-space projection techniques to derive the GLE for filtered observables and to reveal how the GLE parameters are modified by filtering.

There are diverse applications for our filter-projection approach that are graphically illustrated in Fig. 1: i) For constructing coarse-grained models, a low pass filter removes irrelevant fast dynamics of an observable. Our filter-projection approach yields the coarse-grained effective parameters of the GLE (i.e. mass, friction and potential) that exactly describe the long-time observable motion. ii) Conversely, every experimental measurement entails some type of smoothing caused by the finite time response of the measuring apparatus. Our filter projection approach can be used to invert the smoothing and calculate the parameters of the original dynamic process if the filter characteristics are known. iii) For data that is plagued by slow transient or seasonal (i.e. periodic) effects, our filter-projection approach can be used to split the data into the slow and periodic components,

which can be treated by simple deterministic models, and the fast components, which include stochastic effects and for which the GLE approach is ideally suited. Our filter-projection methodology thus is an alternative to non-equilibrium theoretical approaches towards the dynamics of systems with slow transient dynamics.

## II. THE GENERALIZED LANGEVIN EQUATION FOR FILTERED OBSERVABLES

### A. From the Liouville equation to Heisenberg observables

We consider a general time-independent Hamiltonian for a system of  $N$  interacting particles or atoms in three-dimensional space

$$H(\omega) = \sum_{n=1}^N \frac{\mathbf{p}_n^2}{2m_n} + V(\{\mathbf{r}_N\}), \quad (1)$$

where a point in the  $6N$ -dimensional phase space is denoted by  $\omega = (\{\mathbf{r}_N\}, \{\mathbf{p}_N\})$ , which is a  $6N$ -dimensional vector consisting of the Cartesian particle positions  $\{\mathbf{r}_N\}$  and the conjugate momenta  $\{\mathbf{p}_N\}$  and fully specifies the microstate of the system. The Hamiltonian splits into a kinetic and a potential part and  $m_n$  is the mass of particle  $n$ . The potential  $V(\{\mathbf{r}_N\})$  contains all interactions between the particles and includes possible external potentials.

Using the Liouville operator

$$\mathcal{L}(\omega) = \sum_{n=1}^N \sum_{\alpha=x,y,z} \left( \frac{\partial H}{\partial p_n^\alpha} \frac{\partial}{\partial r_n^\alpha} - \frac{\partial H}{\partial r_n^\alpha} \frac{\partial}{\partial p_n^\alpha} \right), \quad (2)$$

the  $6N$ -dimensional Hamilton equation of motion can be compactly written as  $\dot{\omega}(t) = \mathcal{L}(\omega)\omega(t)$ , where  $\omega(t)$  is the phase-space location of the system at time  $t$  and  $\dot{\omega}(t) = d\omega(t)/dt$  is the corresponding phase-space velocity. From the Hamilton equation and since the Liouville operator is time-independent, it follows that the phase space position is propagated in time by the operator exponential  $e^{(t-t_0)\mathcal{L}(\omega)}$ , i.e.,  $e^{(t-t_0)\mathcal{L}(\omega)}\omega(t_0) = \omega(t)$  [44]. Instead of following microstate trajectories in phase space, which is the Lagrangian description of the system dynamics, it is convenient to switch to the Eulerian description and consider the time-dependent probability density distribution as a function of phase space,  $\rho(\omega, t)$ . The density obeys the Liouville equation  $\dot{\rho}(\omega, t) = -\mathcal{L}(\omega)\rho(\omega, t)$ , which has the formal solution  $\rho(t) = e^{-(t-t_0)\mathcal{L}(\omega)}\rho(\omega, t_0)$  with some initial distribution  $\rho(\omega, t_0)$ , which need not be a stationary distribution [44]. A system observable can be generally written as a Schrödinger-type (i.e. time-independent) phase-space function  $B_S(\omega)$ , it can for example represent the position of one particle, its momentum, the center-of-mass position of a group of particles, or the reaction coordinate describing a chemical reaction or the folding of a protein. Since the phase space can

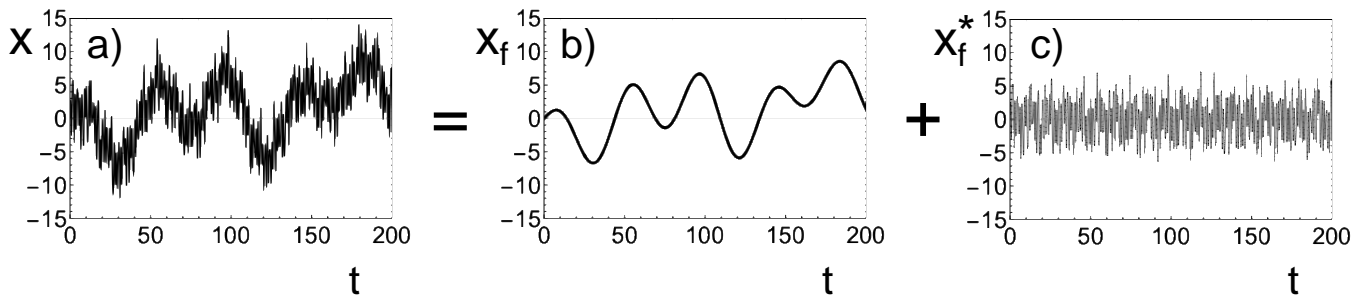


FIG. 1. Graphical illustration of the effect of filtering on a trajectory with multiple time scales. The trajectory  $x(t)$  in a) is by convolution filtering decomposed into the low-pass filtered part  $x_f(t)$  in b) and the high-pass filtered complement  $x_f^*(t)$  in c) such that  $x(t) = x_f(t) + x_f^*(t)$ . In coarse-graining applications one seeks the model that correctly describes the stochastic and equilibrium properties of the filtered component in b). In data-reconstruction applications one would like to infer the dynamics of the unfiltered trajectory in a) from the measured low-pass filtered trajectory in b). Finally, when dealing with systems that contain slow transient dynamics that cannot be fully resolved, the objective is to build models for the high-pass filtered component  $x_f^*(t)$  in c). Our filter-projection approach applies to all these scenarios.

be defined as including the entire universe, so that no external time-dependent external perturbation needs to be taken into account [15, 45],  $B_S(\omega)$  can also represent more complex observables such as the position or state of a living organism, a meteorological or an economical observable. To simplify the notation, we consider a scalar observable but note that our formalism can be straightforwardly extended to multidimensional observables. Using the probability density, the time-dependent expectation value (or mean) of the observable  $B_S(\omega)$  can be written as

$$\begin{aligned} b(t) &\equiv \int d\omega B_S(\omega)\rho(\omega, t) \\ &= \int d\omega B_S(\omega)e^{-(t-t_0)\mathcal{L}(\omega)}\rho(\omega, t_0). \end{aligned} \quad (3)$$

Since the Liouville operator is anti-self adjoint, it follows that [44]

$$\begin{aligned} b(t) &= \int d\omega \rho(\omega, t_0)e^{(t-t_0)\mathcal{L}(\omega)}B_S(\omega) \\ &= \int d\omega \rho(\omega, t_0)B(\omega, t). \end{aligned} \quad (4)$$

In the last step we have defined the Heisenberg observable as

$$B(\omega, t) \equiv e^{(t-t_0)\mathcal{L}(\omega)}B_S(\omega), \quad (5)$$

which is the central object of the projection formalism and of GLEs. Obviously, as follows from Eq. (5), it satisfies the equation of motion

$$\dot{B}(\omega, t) = \mathcal{L}(\omega)B(\omega, t) \quad (6)$$

with the initial condition  $B(\omega, t_0) = B_S(\omega)$ . To understand the meaning of a Heisenberg observable, we for the moment consider the density distribution  $\rho(\omega, t_0) = \delta(\omega - \omega_0)$ , which describes a system that at time  $t_0$  is

in the microstate  $\omega_0$ . Inserting this into Eq. (4), we obtain  $b(t) = B(\omega_0, t)$ . In other words,  $B(\omega_0, t)$  describes the dynamics of an observable for a system that at time  $t = t_0$  was in the microstate  $\omega_0$ , i.e., it describes the temporal evolution of the conditional mean of the observable  $B_S(\omega)$ . It transpires that if we derive an equation of motion for  $B(\omega, t)$ , we have an equation for how this conditional mean changes in time. This is the central idea of projection and of GLEs.

## B. Convolution-filtered Heisenberg observables

In all what follows, we will omit the phase-space argument of the Liouville operator and simply denote it as  $\mathcal{L}$ . Introducing the general convolutional filter function  $f(t)$ , we define the filtered mean of an observable as

$$b_f(t) \equiv \int_{-\infty}^{\infty} ds f(s)b(t-s). \quad (7)$$

Filtering necessarily occurs whenever an experimental measurement is done, but it can also be used purposely to decompose data into separate contributions, to remove unwanted components of time series data or to enhance certain interesting features. Using Eq. (4), the time filtering of the observable mean can be written in terms of a phase-space average as

$$\begin{aligned} b_f(t) &= \int_{-\infty}^{\infty} ds f(s) \int d\omega \rho(\omega, t_0)B(\omega, t-s) \\ &= \int d\omega \rho(\omega, t_0) \int_{-\infty}^{\infty} ds f(s)B(\omega, t-s) \\ &= \int d\omega \rho(\omega, t_0)B_f(\omega, t). \end{aligned} \quad (8)$$

In the last line we defined the filtered Heisenberg observable

$$B_f(\omega, t) \equiv \int_{-\infty}^{\infty} ds f(s) B(\omega, t-s) \quad (9)$$

$$= \int_{-\infty}^{\infty} ds f(s) e^{(t-s-t_0)\mathcal{L}} B_S(\omega), \quad (10)$$

which by construction has the same properties as the unfiltered Heisenberg observable in Eqs. (5) and (6): it is time propagated according to

$$\begin{aligned} e^{t'\mathcal{L}} B_f(\omega, t) &= e^{t'\mathcal{L}} \int_{-\infty}^{\infty} ds f(s) e^{(t-s-t_0)\mathcal{L}} B_S(\omega) \\ &= \int_{-\infty}^{\infty} ds f(s) e^{(t'+t-s-t_0)\mathcal{L}} B_S(\omega) \\ &= B_f(\omega, t'+t) \end{aligned} \quad (11)$$

and it satisfies the equation of motion

$$\dot{B}_f(\omega, t) = \mathcal{L} B_f(\omega, t). \quad (12)$$

Thus, although  $B_f(\omega, t)$  involves a weighted integral over time and thus is not an ordinary observable, i.e., an instantaneously defined phase-space function, its dynamics is identical to that of an ordinary Heisenberg observable. This simple but profound property, which is one of the main results of this paper, will allow us to derive a GLE for the filtered Heisenberg observable  $B_f(\omega, t)$  in exactly the same way as it is commonly done for the ordinary (unfiltered) Heisenberg observable  $B(\omega, t)$ .

### C. Convolution filter examples

In principle any function  $f(t)$  can be employed as a temporal filter, but there are a few particularly useful filter functions. In Fourier space Eq. (9) reads

$$\tilde{B}_f(\omega, \nu) = \tilde{f}(\nu) \tilde{B}(\omega, \nu), \quad (13)$$

where we define Fourier transforms as  $\tilde{f}(\nu) = \int dt e^{-\nu t} f(t)$ . The normalized Gaussian filter with a temporal width  $\lambda$ ,

$$f_{\text{LP}}(t) = e^{-t^2/(2\lambda^2)} (2\pi\lambda^2)^{-1/2}, \quad (14)$$

is a low-pass filter that is commonly used for smoothing experimental and simulation data. Its Fourier transform is given by a Gaussian as well,

$$\tilde{f}_{\text{LP}}(\nu) = e^{-\lambda^2\nu^2/2}. \quad (15)$$

The Gaussian high-pass filter is the complement of the Gaussian low-pass filter and is given by

$$f_{\text{HP}}(t) = \delta(t) - f_{\text{LP}}(t) \quad (16)$$

with the Fourier transform

$$\tilde{f}_{\text{HP}}(\nu) = 1 - e^{-\lambda^2\nu^2/2}. \quad (17)$$

It can be used to eliminate the slow or transient dynamics of a trajectory. The normalized Gaussian band-pass filter

$$f_{\text{BP}}(t, \nu_0) = \frac{\cos(\nu_0 t) e^{-t^2/(2\lambda^2)}}{(2\pi\lambda^2)^{1/2} e^{-\lambda^2\nu_0^2/2}} \quad (18)$$

with its Fourier transform

$$\tilde{f}_{\text{BP}}(\nu, \nu_0) = \frac{e^{-\lambda^2(\nu-\nu_0)^2/2} + e^{-\lambda^2(\nu+\nu_0)^2/2}}{2e^{-\lambda^2\nu_0^2/2}} \quad (19)$$

can be used to perform convolutional Fourier analysis. To illustrate its properties, we consider as an example a cosine function with a finite phase  $\phi$ ,

$$B(\omega, t) = B_0(\omega) \cos(\nu_0' t + \phi), \quad (20)$$

where  $B_0(\omega)$  is an arbitrary phase-space function.  $B(\omega, t)$  has the Fourier transform

$$\tilde{B}(\omega, \nu) = \pi B_0(\omega) (e^{i\phi} \delta(\nu - \nu_0') + e^{-i\phi} \delta(\nu + \nu_0')). \quad (21)$$

According to Eqs. (13) and (18) and after a few intermediate steps, the filtered function can be written in Fourier space as

$$\tilde{B}_f(\omega, \nu, \nu_0) = \tilde{B}(\omega, \nu) \frac{e^{-\lambda^2(\nu_0-\nu_0')^2/2} + e^{-\lambda^2(\nu_0+\nu_0')^2/2}}{2e^{-\lambda^2\nu_0^2/2}} \quad (22)$$

and becomes sharply peaked for a filter frequency  $\nu_0$  around the frequency  $\nu_0'$  of the input function in the limit  $\lambda\nu_0' \gg 1$ . This simple example shows that the Gaussian convolutional band-pass filter projects onto oscillatory contributions in time-series data and thus can be used analogously to ordinary Fourier transformation (which, obviously, does not correspond to a convolution). The Gaussian band-stop filter is the complement of the Gaussian band-pass filter and given by

$$f_{\text{BS}}(t, \nu_0) = \delta(t) - f_{\text{BP}}(t) \quad (23)$$

with the Fourier transform

$$\tilde{f}_{\text{BS}}(\nu, \nu_0) = 1 - \frac{e^{-\lambda^2(\nu-\nu_0)^2/2} + e^{-\lambda^2(\nu+\nu_0)^2/2}}{2e^{-\lambda^2\nu_0^2/2}}. \quad (24)$$

It can be used to eliminate oscillatory dynamics with oscillation frequency  $\nu_0$  in time-series data. Of course, one can apply an arbitrary combination of filter functions onto time-series data and the resulting function behaves as a regular phase-space observable, as explained in Sect. II B.

#### D. Derivation of the GLE for convolution-filtered Heisenberg observables

Using the definition Eq. (9), we decompose the unfiltered Heisenberg observable  $B(\omega, t)$  into the filtered Heisenberg observable  $B_f(\omega, t)$  and its complement  $B_f^*(\omega, t)$  according to

$$B(\omega, t) = B_f(\omega, t) + B_f^*(\omega, t). \quad (25)$$

Note that this decomposition is exact and can be viewed as the definition of the complement. By adding many convolution-filtered Heisenberg observables according to  $B_f(\omega, t) = \sum_i B_f^i(\omega, t)$ , where the  $i$  numbers different convolution filters, we can apply multiple low-pass, high-pass, band-pass and band-stop filters on the data. According to Eq. (25), the acceleration of the unfiltered Heisenberg observable can be decomposed as

$$\ddot{B}(\omega, t) = \ddot{B}_f(\omega, t) + \ddot{B}_f^*(\omega, t). \quad (26)$$

As a matter of fact, one can analyze the two parts on the right side of Eq. (26) separately and using different types of theoretical description. For the example of a high-pass filter, one could use a stochastic description for the high-pass filtered part  $B_f(\omega, t)$ , which contains the fast fluctuations, while the low-pass complement  $B_f^*(\omega, t)$ , which contains the slow components, could be described by a deterministic model. In the following we will apply the projection formalism on  $\ddot{B}_f(\omega, t)$  but stress that projection can be equally well applied on the complementary part  $\ddot{B}_f^*(\omega, t)$ .

Here we follow standard procedures [44]. We introduce a projection operator  $\mathcal{P}$  that acts on phase space functions and its complementary operator  $\mathcal{Q}$  via the relation  $1 = \mathcal{Q} + \mathcal{P}$ . Inserting this unit operator into the time propagator relation Eq. (11) and using Eq. (12), we obtain

$$\begin{aligned} \ddot{B}_f(\omega, t) &= e^{(t-t_P)\mathcal{L}}(\mathcal{P} + \mathcal{Q})\mathcal{L}^2 B_f(\omega, t_P) \\ &= e^{(t-t_P)\mathcal{L}}\mathcal{P}\mathcal{L}^2 B_f(\omega, t_P) + e^{(t-t_P)\mathcal{L}}\mathcal{Q}\mathcal{L}^2 B_f(\omega, t_P), \end{aligned} \quad (27)$$

where  $t_P$  defines the time at which the projection is performed, which in principle can differ from the time  $t_0$  at which the time propagation of the Heisenberg variable in Eq. (11) starts. The projection operators  $\mathcal{Q}$  and  $\mathcal{P}$  in general depend on the projection time  $t_P$  (which is not explicitly written out) but not on the time  $t$ . This allows us to use the standard Dyson operator decomposition [46–48] for the propagator  $e^{(t-t_P)\mathcal{L}}$

$$e^{(t-t_P)\mathcal{L}} = e^{(t-t_P)\mathcal{Q}\mathcal{L}} + \int_0^{t-t_P} ds e^{(t-t_P-s)\mathcal{L}}\mathcal{P}\mathcal{L}e^{s\mathcal{Q}\mathcal{L}}. \quad (28)$$

Inserting this decomposition into the second term on the right hand side in Eq. (27), we obtain the GLE in general

form

$$\begin{aligned} \ddot{B}_f(\omega, t) &= e^{(t-t_P)\mathcal{L}}\mathcal{P}\mathcal{L}^2 B_f(\omega, t_P) + F(\omega, t) \\ &+ \int_0^{t-t_P} ds e^{(t-t_P-s)\mathcal{L}}\mathcal{P}\mathcal{L}F(\omega, s + t_P), \end{aligned} \quad (29)$$

where the complementary force is given by

$$F(\omega, t) \equiv e^{(t-t_P)\mathcal{Q}\mathcal{L}}\mathcal{Q}\mathcal{L}^2 B_f(\omega, t_P). \quad (30)$$

The first term on the right-hand side in Eq. (29) will turn out to represent the conservative force from a potential, the third term represents non-Markovian friction effects and the force  $F(\omega, t)$  represents all effects that are not included in the other two terms.  $F(\omega, t)$  is a function of phase space and evolves in the complementary space, i.e. it satisfies  $\mathcal{P}F(\omega, t) = 0$  (as will be shown further below).

Clearly, the explicit form of Eq. (29) depends on the specific form of the projection operator  $\mathcal{P}$ . Here we choose the Mori projection, because it is straightforward to implement and for the derivation of the filtering effects based on two-point correlations functions is exact, as we will discuss below. We note that our filter-projection approach can also be used in conjunction with hybrid projection operators for which the resulting GLE explicitly contains a non-linear potential of mean force [49–51]. The Mori projection using  $B_f(\omega, t_P)$  as a projection function and applied on a general Heisenberg observable  $A(\omega, t)$  is given by [31, 50]

$$\begin{aligned} \mathcal{P}A(\omega, t) &= \langle A(\omega, t) \rangle + \frac{\langle A(\omega, t)\mathcal{L}B_f(\omega, t_P) \rangle}{\langle (\mathcal{L}B_f(\omega, t_P))^2 \rangle} \mathcal{L}B_f(\omega, t_P) \\ &+ \frac{\langle A(\omega, t)(B_f(\omega, t_P) - \langle B_f \rangle) \rangle}{\langle (B_f(\omega, t_P) - \langle B_f \rangle)^2 \rangle} (B_f(\omega, t_P) - \langle B_f \rangle). \end{aligned} \quad (31)$$

We define the expectation value of an arbitrary phase-space function  $X(\omega)$  with respect to a time-independent projection distribution  $\rho_P(\omega)$  as

$$\langle X(\omega) \rangle = \int d\omega X(\omega)\rho_P(\omega), \quad (32)$$

which we here take to be the normalized equilibrium canonical distribution  $\rho_P(\omega) = e^{-H(\omega)/(k_B T)}/Z$ , where  $Z$  is the partition function. For this stationary projection distribution the average  $\langle B_f \rangle = \langle B_f(\omega, t_P) \rangle$  is independent of time. The Mori projection in Eq. (31) projects onto a constant, the filtered observable  $B_f(\omega, t_P)$  and its time derivative  $\mathcal{L}B_f(\omega, t_P)$  at time  $t_P$ , the projection time. Thus, the projection in Eq. (31) maps any observable  $A(\omega, t)$  onto the subspace of all functions linear in the observables  $1$ ,  $B_f(\omega, t_P)$  and  $\mathcal{L}B_f(\omega, t_P)$ , meaning that  $\mathcal{P}1 = 1$ ,  $\mathcal{P}B_f(\omega, t_P) = B_f(\omega, t_P)$  and  $\mathcal{P}\mathcal{L}B_f(\omega, t_P) = \mathcal{L}B_f(\omega, t_P)$ . From this follows immediately that  $\mathcal{Q}1 = \mathcal{Q}B_f(\omega, t_P) = \mathcal{Q}\mathcal{L}B_f(\omega, t_P) = 0$ , which is a property that will become important later on.

The Mori projection is linear, i.e., for two arbitrary observables  $A(\omega, t)$  and  $C(\omega, t')$  it satisfies  $\mathcal{P}(c_1 A(\omega, t) +$

$c_2 C(\omega, t') = c_1 \mathcal{P}A(\omega, t) + c_2 \mathcal{P}C(\omega, t')$ , it is idempotent, i.e.,  $\mathcal{P}^2 = \mathcal{P}$ , and it is self-adjoint, i.e. it satisfies the relation

$$\langle A(\omega, t) \mathcal{P}C(\omega, t') \rangle = \langle C(\omega, t') \mathcal{P}A(\omega, t) \rangle. \quad (33)$$

From these properties it follows that the complementary projection operator  $\mathcal{Q} = 1 - \mathcal{P}$  is also linear, idempotent and self-adjoint. Thus,  $\mathcal{P}$  and  $\mathcal{Q}$  are orthogonal to each other, i.e.  $\mathcal{P}\mathcal{Q} = 0 = \mathcal{Q}\mathcal{P}$  [45].

Using all these properties, the GLE Eq. (29) takes the form [31, 44]

$$\begin{aligned} \ddot{B}_f(\omega, t) &= -K_f(B_f(\omega, t) - \langle B_f \rangle) + F(\omega, t) \\ &\quad - \int_0^{t-t_P} ds \Gamma_f(s) \dot{B}_f(\omega, t-s), \end{aligned} \quad (34)$$

details of the derivation are shown in Appendix A. The parameter  $K_f$ , which corresponds to the potential stiffness divided by the effective mass, is given by

$$K_f = \frac{\langle (\mathcal{L}B_f(\omega, t_P))^2 \rangle}{\langle (B_f(\omega, t_P) - \langle B_f \rangle)^2 \rangle} \quad (35)$$

and the memory friction kernel is given by

$$\Gamma_f(s) = \frac{\langle F(\omega, t_P) F(\omega, s+t_P) \rangle}{\langle (\mathcal{L}B_f(\omega, t_P))^2 \rangle} = \frac{\langle F(\omega, 0) F(\omega, s) \rangle}{\langle (\mathcal{L}B_f(\omega, t_P))^2 \rangle}. \quad (36)$$

Eq. (34) is an exact decomposition of the Liouville equation into three terms, the first term is a force due to a quadratic potential, the third term accounts for linear non-Markovian friction and depends on the memory kernel  $\Gamma_f(s)$ , which is related via Eq. (36) to the second moment of the force  $F(\omega, t)$ , defined in Eq. (30). In particular, eq. (34) is exact and time-reversible, as are the underlying Hamilton and Liouville equations. The explicit form of the memory function can be computed for simple model systems, as will be demonstrated later on. Note that the force  $F(\omega, t)$  can be extracted from simulation or experimental data by different techniques [49, 52, 53]. Due to the specific form of the Mori projection in Eq. (31), several expectation values involving the force vanish, namely  $\langle F(\omega, t) \rangle = \langle F(\omega, t) B_f(\omega, t_P) \rangle = \langle F(\omega, t) \mathcal{L}B_f(\omega, t_P) \rangle = 0$ , which are important properties for extracting GLE parameters from time-series data.

For practical applications, one typically models the force  $F(\omega, t)$  as a stochastic process with zero mean and a second moment given by Eq. (36), higher-order moments of  $F(\omega, t)$  are typically neglected and the distribution of  $F(\omega, t)$  is assumed to be Gaussian, which is valid for the calculation of two-point correlation functions. For non-linear systems and if one is interested in higher-order correlations, however, this assumption can not hold, since  $F(\omega, t)$  is the only term in the GLE that accounts for non-linearities. Thus, imposing  $F(\omega, t)$  to be a Gaussian variable can become a bad approximation for non-linear systems, which reflects a fundamental short-coming of

the Mori projection scheme in conjunction with replacing  $F(\omega, t)$  by a random Gaussian process. Alternative methods to derive GLEs with non-linear potential and friction terms have been recently proposed [49–51, 54]. We stay here with the Mori scheme because it simplifies analytical calculations and is exact for our calculations of two-point correlations. We note that high-pass filtering produces data that is Gaussian to a very good approximation.

### III. DYNAMIC PROPERTIES OF FILTERED TRAJECTORIES

#### A. Parameters of the GLE for filtered observables

We now interpret the GLE in Eq. (34) for the phase-space dependent filtered Heisenberg observable  $B_f(\omega, t)$  as a stochastic equation. For a more stream-lined notation, we skip the phase-space dependence and define the filtered observable by subtracting its mean as

$$x_f(t) = B_f(\omega, t) - \langle B_f \rangle. \quad (37)$$

We also shift the projection time into the far past,  $t_P \rightarrow -\infty$ , define the memory kernel to be causal or single-sided, i.e.  $\Gamma_f(t) = 0$  for  $t < 0$ , and define a stochastic random force as  $F_R(t) = F(\omega, t)$ . The GLE reads

$$\ddot{x}_f(t) = -K_f x_f(t) + F_R(t) - \int_{-\infty}^{\infty} ds \Gamma_f(s) \dot{x}_f(t-s), \quad (38)$$

where the potential parameter is, following Eq. (35), given by

$$K_f = \frac{\langle \dot{x}_f^2 \rangle}{\langle x_f^2 \rangle} \quad (39)$$

and the memory friction kernel is, following Eq. (36), given by

$$\Gamma_f(t) = \theta(t) \frac{\langle F_R(0) F_R(t) \rangle}{\langle \dot{x}_f^2 \rangle} \quad (40)$$

where  $\theta(t)$  defines the Heavyside function and the mean-squared velocity  $\langle \dot{x}^2 \rangle$  would, for a standard equilibrium observable and according to the equipartition theorem, correspond to the thermal energy divided by the effective mass. The force  $F_R(t)$  is characterized by its second moment according to Eq. (40), while its first moment vanishes,  $\langle F_R(t) \rangle = 0$ , as explained before. This, however, does not mean that the random force is necessarily Gaussian. Note that from now on, all expectation values are defined as averages with respect to the random force distribution. This reinterpretation of the GLE in Eq. (34) as a stochastic integro-differential equation simplifies the notation significantly and is exact as long as care is taken

to relegate all phase-space dependencies into the random force  $F_R(t)$ .

By Fourier transformation, Eq. (38) can be solved in terms of the linear-response relation as

$$\tilde{x}_f(\nu) = \tilde{\chi}_f(\nu)\tilde{F}_R(\nu), \quad (41)$$

where the response function is given as

$$\tilde{\chi}_f(\nu) = \left[ K_f - \nu^2 + \nu\tilde{\Gamma}_f(\nu) \right]^{-1}. \quad (42)$$

We define the filtered two-point positional autocorrelation function as

$$C_{xx}^f(t) = \langle x_f(t)x_f(t+t') \rangle, \quad (43)$$

the Fourier transform of which reads

$$\begin{aligned} \tilde{C}_{xx}^f(\nu) &= \int \frac{dt'}{2\pi} e^{it'(\nu+\nu')} \langle \tilde{x}_f(\nu)\tilde{x}_f(\nu') \rangle \\ &= \int \frac{dt'}{2\pi} e^{it'(\nu+\nu')} \tilde{\chi}_f(\nu)\tilde{\chi}_f(\nu') \langle \tilde{F}_R(\nu)\tilde{F}_R(\nu') \rangle \end{aligned} \quad (44)$$

where in the last step we used Eq. (41). The random-force autocorrelation in Fourier space follows from Eq. (40) as

$$\langle \tilde{F}_R(\nu)\tilde{F}_R(\nu') \rangle = 2\pi\delta(\nu+\nu')\langle \dot{x}_f^2 \rangle \left[ \tilde{\Gamma}_f(\nu) + \tilde{\Gamma}_f(\nu') \right]. \quad (45)$$

Combining Eqs. (44) and (45) we obtain

$$\begin{aligned} \tilde{C}_{xx}^f(\nu) &= \langle \dot{x}_f^2 \rangle \tilde{\chi}_f(\nu)\tilde{\chi}_f(-\nu) \left[ \tilde{\Gamma}_f(\nu) + \tilde{\Gamma}_f(-\nu) \right] \\ &= \frac{\langle \dot{x}_f^2 \rangle}{\nu} [\tilde{\chi}_f(-\nu) - \tilde{\chi}_f(\nu)], \end{aligned} \quad (46)$$

where in the last step we used Eq. (42). Eq. (46) forms the starting point for a few further derivations and is exactly produced by the Mori GLE. First, we multiply Eq. (46) by  $\nu$  to obtain

$$\tilde{C}_{x\dot{x}}^f(\nu) \equiv \nu\tilde{C}_{xx}^f(\nu) = \langle \dot{x}_f^2 \rangle [\tilde{\chi}_f(-\nu) - \tilde{\chi}_f(\nu)], \quad (47)$$

where  $\tilde{C}_{x\dot{x}}^f(\nu)$  is the Fourier transform of the derivative of the positional autocorrelation function  $C_{x\dot{x}}^f(t) \equiv dC_{xx}^f(t)/dt = \langle x_f(0)\dot{x}_f(t) \rangle$ . The right-hand side of Eq. (47) splits into a causal part,  $\tilde{\chi}_f(\nu)$ , and an anticausal part,  $\tilde{\chi}_f(-\nu)$ , therefore we can also split the left-hand side into causal and anticausal parts and finally obtain

$$\tilde{C}_{x\dot{x}}^{+f}(\nu) = -\langle \dot{x}_f^2 \rangle \tilde{\chi}_f(\nu), \quad (48)$$

where  $\tilde{C}_{x\dot{x}}^{+f}(\nu)$  is the Fourier transform of the single-sided correlation function,  $C_{x\dot{x}}^{+f}(t) = \theta(t)C_{x\dot{x}}^f(t)$ . Eq. (48) is the Fourier transform of the fluctuation dissipation theorem [44] and one can use it to extract all parameters of the

filtered GLE from filtered time series data. To see this we combine Eqs. (48) and (42) to obtain

$$-\frac{\langle \dot{x}_f^2 \rangle}{\tilde{C}_{x\dot{x}}^{+f}(\nu)} = K_f - \nu^2 - \nu\tilde{\Gamma}_f''(\nu) + \nu\tilde{\Gamma}_f'(\nu), \quad (49)$$

where we split the memory function into its real and imaginary parts according to  $\tilde{\Gamma}_f(\nu) = \tilde{\Gamma}_f'(\nu) + i\tilde{\Gamma}_f''(\nu)$ . It transpires that the real and imaginary parts of the memory function are determined by

$$\Gamma_f'(\nu) = -\left( \frac{\langle \dot{x}_f^2 \rangle}{\nu\tilde{C}_{x\dot{x}}^{+f}(\nu)} \right)'', \quad (50a)$$

$$\Gamma_f''(\nu) = \frac{K_f}{\nu} - \nu + \left( \frac{\langle \dot{x}_f^2 \rangle}{\nu\tilde{C}_{x\dot{x}}^{+f}(\nu)} \right)'. \quad (50b)$$

The potential parameter  $K_f$  follows from Eq. (39) or, alternatively, from Eq. (49) in the zero-frequency limit as

$$K_f = -\frac{\langle \dot{x}_f^2 \rangle}{\tilde{C}_{x\dot{x}}^{+f}(0)} = \frac{\langle \dot{x}_f^2 \rangle}{\langle x_f^2 \rangle}, \quad (51)$$

where we used that the Fourier transform of the memory function is finite in the zero frequency limit. In numerical applications, Eq. (51) can serve as a check on the accuracy of the numerical determination of  $\tilde{C}_{x\dot{x}}^{+f}(\nu)$ . Eqs. (50) and (51) can be used to extract all parameters of the filtered GLE in Eq. (38) from a filtered trajectory, since  $\tilde{C}_{x\dot{x}}^{+f}(\nu)$  and the expectation values  $\langle x_f^2 \rangle$  and  $\langle \dot{x}_f^2 \rangle$  can be directly evaluated from time-series data.

Let us derive a second useful result from Eq. (46). Since  $\chi_f(t)$  is a real function, it follows that  $\tilde{\chi}_f'(\nu) = \tilde{\chi}_f'(-\nu)$  and  $\tilde{\chi}_f''(\nu) = -\tilde{\chi}_f''(-\nu)$ . Using this in Eq. (46), we obtain

$$\tilde{C}_{xx}^f(\nu) = -\frac{2\langle \dot{x}_f^2 \rangle \tilde{\chi}_f''(\nu)}{\nu}, \quad (52)$$

which is an alternative formulation of the fluctuation-dissipation theorem in Fourier space [44]. In the zero-frequency limit we obtain from Eq. (52)

$$\tilde{C}_{xx}^f(0) = \frac{2\langle \dot{x}_f^2 \rangle \tilde{\Gamma}_f(0)}{K_f^2} = \frac{2\langle x_f^2 \rangle \tilde{\Gamma}_f(0)}{K_f}, \quad (53)$$

where we used Eqs. (42) and (39) and  $\tilde{\Gamma}_f(0)$ , the integral over the memory function, is the friction coefficient. For unconfined systems with  $K_f = 0$ ,  $\tilde{\Gamma}_f(0)$  can be obtained from Eq. (52) using the velocity autocorrelation function  $C_{x\dot{x}}^f(t) \equiv \langle \dot{x}_f(0)\dot{x}_f(t) \rangle = -d^2C_{xx}^f(t)/dt^2$  as

$$\tilde{C}_{x\dot{x}}^f(0) = \frac{2\langle \dot{x}_f^2 \rangle}{\tilde{\Gamma}_f(0)}, \quad (54)$$

which corresponds to the standard relation between the integral over the velocity autocorrelation function,  $\tilde{C}_{x\dot{x}}^f(0)$ , and the diffusion constant [44]. Relations Eqs. (53) and (54) can be used to obtain the friction coefficient  $\tilde{\Gamma}_f(0)$  from filtered trajectory data.

## B. Mapping between filtered and unfiltered GLE parameters

We now discuss the mapping between the filtered observable  $x_f(t)$ , described by the GLE in Eq. (38), and the unfiltered observable, denoted as  $x(t)$  and which we describe by the same GLE but with different (i.e. unfiltered) parameters  $K$ ,  $\Gamma(t)$  and an unfiltered random force that is characterized by its second moment according to Eq. (40) where  $\langle \dot{x}_f^2 \rangle$  is replaced by  $\langle \dot{x}^2 \rangle$ . Similarly to Eq. (13), the relation between  $x_f(t)$  and  $x(t)$  is given by

$$\tilde{x}_f(\nu) = \tilde{f}(\nu)\tilde{x}(\nu). \quad (55)$$

The question is, given the parameters of the GLE for the unfiltered observable, what are the parameters of the GLE for the filtered observable, or vice versa. As turns out, this is a rather non-trivial question.

First, using Eq. (55), the positional autocorrelation function for the filtered observable  $x_f(t)$  in Eq. (44) can be written as

$$\begin{aligned} \tilde{C}_{xx}^f(\nu) &= \int \frac{dt'}{2\pi} e^{it'(\nu+\nu')} \tilde{f}(\nu)\tilde{f}(\nu') \langle \tilde{x}(\nu)\tilde{x}(\nu') \rangle \\ &= \tilde{f}(\nu)\tilde{f}(-\nu)\tilde{C}_{xx}(\nu), \end{aligned} \quad (56)$$

where we followed the same steps leading to Eq. (46). This relation connects the autocorrelations for the filtered observable  $\tilde{C}_{xx}^f(\nu)$  and the unfiltered observable  $\tilde{C}_{xx}(\nu)$  and furnishes the central relation for understanding the effect of filtering on the system dynamics.

Combining Eqs. (53) and (56) leads to

$$\frac{\langle \dot{x}_f^2 \rangle \tilde{\Gamma}_f(0)}{K_f^2} = \frac{\tilde{f}^2(0)\langle \dot{x}^2 \rangle \tilde{\Gamma}(0)}{K^2}, \quad (57)$$

which is a relation between the parameters of the GLEs describing the filtered and unfiltered observables. In the following sections we will disentangle the filtering effect on the GLE parameters.

### 1. Extracting filtered parameters from unfiltered trajectories

We now combine Eqs. (47) and (56) to obtain

$$\begin{aligned} \tilde{\chi}_f(-\nu) - \tilde{\chi}_f(\nu) &= \frac{\tilde{f}(\nu)\tilde{f}(-\nu)\nu\tilde{C}_{xx}(\nu)}{\langle \dot{x}_f^2 \rangle} \\ &\equiv \frac{\tilde{C}_{u \rightarrow f}(\nu)}{\langle \dot{x}_f^2 \rangle}. \end{aligned} \quad (58)$$

By defining the the single-sided time-domain function  $C_{u \rightarrow f}^+(t) = \theta(t)C_{u \rightarrow f}(t)$ , where  $C_{u \rightarrow f}(t)$  is the back Fourier transform of  $\tilde{C}_{u \rightarrow f}(\nu) \equiv \tilde{f}(\nu)\tilde{f}(-\nu)\nu\tilde{C}_{xx}(\nu)$ , we obtain by splitting Eq. (58) into its causal and anticausal

parts

$$-\frac{\langle \dot{x}_f^2 \rangle}{\tilde{C}_{u \rightarrow f}^+(\nu)} = \tilde{\chi}_f^{-1}(\nu) = K_f - \nu^2 - \nu\tilde{\Gamma}_f''(\nu) + \nu\tilde{\Gamma}_f'(\nu). \quad (59)$$

Following the same strategy leading to Eq. (50) we obtain

$$\tilde{\Gamma}_f'(\nu) = - \left( \frac{\langle \dot{x}_f^2 \rangle}{\nu\tilde{C}_{u \rightarrow f}^+(\nu)} \right)'' \quad (60a)$$

$$\tilde{\Gamma}_f''(\nu) = \frac{K_f}{\nu} - \nu + \left( \frac{\langle \dot{x}_f^2 \rangle}{\nu\tilde{C}_{u \rightarrow f}^+(\nu)} \right)'. \quad (60b)$$

From Eq. (56) the mean-squared position and velocity follow as

$$\langle x_f^2 \rangle = \int \frac{d\nu}{2\pi} \tilde{C}_{xx}^f(\nu) = \int \frac{d\nu}{2\pi} \tilde{f}(\nu)\tilde{f}(-\nu)\tilde{C}_{xx}(\nu) \quad (61a)$$

$$\langle \dot{x}_f^2 \rangle = \int \frac{d\nu}{2\pi} \nu^2 \tilde{C}_{xx}^f(\nu) = \int \frac{d\nu}{2\pi} \nu^2 \tilde{f}(\nu)\tilde{f}(-\nu)\tilde{C}_{xx}(\nu). \quad (61b)$$

The stiffness  $K_f$  defined in Eq. (39) follows by dividing the results in Eq. (61). Together, thus, Eqs. (60) and (61) allow us to calculate all parameters of the GLE for the filtered observable,  $K_f$ ,  $\Gamma_f(t)$ ,  $\langle \dot{x}_f^2 \rangle$  and, using Eq. (57), also the friction coefficient  $\tilde{\Gamma}_f(0)$  from the trajectory of the unfiltered observable, the only additional input required is the Fourier transform of the filter function  $\tilde{f}(\nu)$ . These formulas thus determine all parameters of the time-coarse grained GLE, as will be further discussed below.

### 2. Extracting unfiltered parameters from filtered trajectories

The other direction is also important for applications, namely reconstructing the parameters of the GLE for unfiltered observables from filtered trajectories. This is relevant when trajectories of a systems are measured using an experimental device that filters the read out, which is true for any experimental measurement. The derivation is completely analogous to the one in the previous section, except that filtered and unfiltered functions are reversed and  $\tilde{f}(\nu)$  is replaced by  $1/\tilde{f}(\nu)$ . Defining in analogy to Eq. (58) the function

$$\tilde{C}_{f \rightarrow u}(\nu) = \frac{\nu\tilde{C}_{xx}^f(\nu)}{\tilde{f}(\nu)\tilde{f}(-\nu)} \quad (62)$$

we obtain

$$\tilde{\Gamma}'(\nu) = - \left( \frac{\langle \dot{x}^2 \rangle}{\nu\tilde{C}_{f \rightarrow u}^+(\nu)} \right)'' \quad (63a)$$

$$\tilde{\Gamma}''(\nu) = \frac{K}{\nu} - \nu + \left( \frac{\langle \dot{x}^2 \rangle}{\nu\tilde{C}_{f \rightarrow u}^+(\nu)} \right)', \quad (63b)$$

where  $\tilde{C}_{f \rightarrow u}^+(\nu)$  is the Fourier transform of the single-sided time-domain function  $C_{f \rightarrow u}^+(t) = \theta(t)C_{f \rightarrow u}(t)$  and  $C_{f \rightarrow u}(t)$  is the back Fourier transform of  $\tilde{C}_{f \rightarrow u}(\nu)$ . Furthermore, from Eq. (56) we find

$$\langle x^2 \rangle = \int \frac{d\nu}{2\pi} \tilde{C}_{xx}(\nu) = \int \frac{d\nu}{2\pi} \frac{\tilde{C}_{xx}^f(\nu)}{\tilde{f}(\nu)\tilde{f}(-\nu)} \quad (64a)$$

$$\langle \dot{x}^2 \rangle = \int \frac{d\nu}{2\pi} \nu^2 \tilde{C}_{xx}(\nu) = \int \frac{d\nu}{2\pi} \frac{\nu^2 \tilde{C}_{xx}^f(\nu)}{\tilde{f}(\nu)\tilde{f}(-\nu)}. \quad (64b)$$

The potential parameter  $K = \langle \dot{x}^2 \rangle / \langle x^2 \rangle$  for the unfiltered GLE, defined in analogy to Eq. (39) for the filtered observable, follows from the results in Eq. (64). Together, thus, Eqs. (63) and (64) allow to calculate all parameters of the GLE for the unfiltered observable,  $K$ ,  $\Gamma(t)$ ,  $\langle \dot{x}^2 \rangle$  and, using Eq. (57), also the friction coefficient  $\tilde{\Gamma}(0)$  from the trajectory of the filtered observable, if the Fourier transform of the filter function  $\tilde{f}(\nu)$  is known.

### C. Analytical results for Debye filter

The mapping between filtered and unfiltered dynamics derived so far involves Fourier transforms of the convolution of the two-point correlation function with the filter function, which for general filter functions must be done numerically. For the case of a Debye filter, defined as

$$\tilde{f}(\nu)\tilde{f}(-\nu) = \frac{1}{1 + \lambda^2\nu^2}, \quad (65)$$

some closed-form results can be obtained by pole analysis. In the time domain, one possible realization of this filter is  $f(t) = \theta(-t)e^{t/\lambda}/\lambda$  and corresponds to a single-sided normalized exponential low-pass filter with the decay time  $\lambda$ . By residual calculus, the details of which are shown in Appendix B, the integrals in Eq. (61) can be done with the results

$$\langle x_f^2 \rangle = \langle x^2 \rangle \left[ \frac{1 + \lambda\tilde{\Gamma}(-i/\lambda)}{1 + \lambda\tilde{\Gamma}(-i/\lambda) + \lambda^2 K} \right], \quad (66a)$$

$$\langle \dot{x}_f^2 \rangle = \langle \dot{x}^2 \rangle \left[ \frac{1}{1 + \lambda\tilde{\Gamma}(-i/\lambda) + \lambda^2 K} \right], \quad (66b)$$

where  $\tilde{\Gamma}(-i/\lambda)$  is the kernel Laplace transform, which is a real function. It is seen that the mean-squared position decreases due to Debye filtering. Also the mean-squared velocity goes down due to Debye filtering for memory functions with a positive Laplace transform, which is the typical scenario. Interestingly, the potential parameter of the filtered observable

$$K_f = \frac{\langle \dot{x}_f^2 \rangle}{\langle x_f^2 \rangle} = \frac{K}{1 + \lambda\tilde{\Gamma}(-i/\lambda)} \quad (67)$$

goes down for memory functions with a positive Laplace transform. This means that the effect of Debye

filtering on the mean-squared velocity dominates over the filtering effect on the mean-squared position. If we were dealing with a standard equilibrium system, we would say that the filtering effect on the effective mass, defined by the equipartition theorem as  $m_{\text{eff}}^f = k_B T / \langle \dot{x}_f^2 \rangle$ , is more important than the filtering effect on the bare harmonic potential strength, which is given by  $k_B T / \langle x_f^2 \rangle$ .

Combining Eqs. (57), (66), (67) we obtain for the Debye-filtered friction coefficient

$$\tilde{\Gamma}_f(0) = \tilde{\Gamma}(0) \frac{1 + \lambda\tilde{\Gamma}(-i/\lambda) + \lambda^2 K}{(1 + \lambda\tilde{\Gamma}(-i/\lambda))^2}. \quad (68)$$

Interestingly, we see that depending on the values of the memory function  $\tilde{\Gamma}(-i/\lambda)$  and the potential stiffness  $K$  of the unfiltered system, the Debye-filtered friction coefficient  $\tilde{\Gamma}_f(0)$  can go up or down compared to the unfiltered friction coefficient  $\tilde{\Gamma}(0)$ . Only for an unconfined system, i.e. for  $K = 0$ , it is clear that the Debye-filtered friction coefficient  $\tilde{\Gamma}_f(0)$  goes down.

What do these results mean for the dynamics of the filtered system? Similar to the overdamped harmonic oscillator, two characteristic time scales are relevant besides the memory time, which we will discuss in the next section: The persistence time  $\tau_{\text{per}}^f = 1/\tilde{\Gamma}_f(0)$ , which is the time over which the filtered observable moves ballistically, and the relaxation time  $\tau_{\text{rel}}^f = \tilde{\Gamma}_f(0)/K_f$ , which measures how quickly the filtered observable relaxes from an excursion. From the results for  $\tilde{\Gamma}_f(0)$  and  $K_f$  in Eqs. (67) and (68) we infer that  $\tau_{\text{per}}^f$  can increase or decrease due to Debye filtering, but the relaxation time  $\tau_{\text{rel}}^f$  strictly increases due to Debye filtering. This is relevant for coarse-graining procedures, because it means that the relaxation time of a low-pass filtered coarse-grained observable will go up.

As a side remark, we add that Eqs. (66) and (67) can be used as an alternative and presumably numerically rather stable method to extract the Laplace-transformed memory kernel  $\tilde{\Gamma}(-i/\lambda)$  from simulation or experimental data by applying a Debye filter on the trajectory.

### D. Analytical result for the memory function induced by Debye filtering of Markovian trajectories

Even for a Debye filter, the calculation of the friction kernel that describes the filtered observable for a general unfiltered system according to Eq. (60) is analytically prohibitive. Here we further simplify the problem by assuming that the unfiltered trajectory comes from a Markovian system, i.e., the friction kernel describing the unfiltered observable is given by a delta function as  $\Gamma(t) = 2\gamma\delta(t)$ . Thus the response function of the unfiltered system is according to Eq. (42) given by

$$\tilde{\chi}(\nu) = [K - \nu^2 + i\nu\gamma]^{-1}. \quad (69)$$

Following Eq. (46), the unfiltered two-point positional auto-correlation function is given as

$$\tilde{C}_{xx}(\nu) = \frac{\langle \dot{x}^2 \rangle}{i\nu} [\tilde{\chi}(-\nu) - \tilde{\chi}(\nu)]. \quad (70)$$

Combining Eqs. (42), (46), (56), (65), (69) and (70) we arrive at the implicit equation that determines the parameters of the Debye-filtered GLE, namely  $\langle \dot{x}_f^2 \rangle$ ,  $K_f$  and  $\tilde{\Gamma}_f(\nu)$ , in terms of the parameters of the unfiltered GLE, namely  $\langle \dot{x}^2 \rangle$ ,  $K$  and  $\gamma$ , which reads

$$\langle \dot{x}_f^2 \rangle \left[ \frac{1}{K_f - \nu^2 - i\nu\tilde{\Gamma}_f(-\nu)} - \frac{1}{K_f - \nu^2 + i\nu\tilde{\Gamma}_f(\nu)} \right] = \frac{\langle \dot{x}^2 \rangle}{1 + \lambda^2\nu^2} \left[ \frac{1}{K - \nu^2 - i\nu\gamma} - \frac{1}{K - \nu^2 + i\nu\gamma} \right]. \quad (71)$$

Note that the filtering mixes anticausal and causal poles on the right-hand side of the equation. Separating the 6 poles of the equation into terms that are purely causal and anticausal, the details of the calculation are shown in Appendix C, yields the final results

$$\frac{\langle \dot{x}_f^2 \rangle}{\langle \dot{x}^2 \rangle} = \frac{1 + \lambda\gamma}{1 + \lambda\gamma + \lambda^2 K} \quad (72a)$$

$$\frac{\langle \dot{x}_f^2 \rangle}{\langle \dot{x}^2 \rangle} = \frac{1}{1 + \lambda\gamma + \lambda^2 K} \quad (72b)$$

$$K_f = \frac{\langle \dot{x}_f^2 \rangle}{\langle \dot{x}^2 \rangle} = \frac{K}{1 + \lambda\gamma}, \quad (72c)$$

which agree with the results in the preceding section for a general non-Markovian unfiltered system Eqs. (66) and (67). It is seen that both mean-squared position and mean-squared velocity go down due to Debye-filtering in a way so that the filtered potential parameter  $K_f$  goes also down. The closed-form result for the memory kernel of the filtered variable reads

$$\tilde{\Gamma}_f(\nu) = \frac{\gamma_f}{1 + i\tau_f\nu}, \quad (73)$$

which means that Debye-filtering induces an exponentially decaying memory kernel, which in the time domain reads

$$\Gamma_f(t) = \frac{\gamma_f}{\tau_f} e^{-t/\tau_f}, \quad (74)$$

with the effective friction and memory time given by

$$\gamma_f = \frac{\gamma(1 + \lambda\gamma + \lambda^2 K)}{(1 + \lambda\gamma)^2}, \quad (75a)$$

$$\tau_f = \frac{\lambda}{1 + \lambda\gamma}. \quad (75b)$$

We remark that the result for the friction coefficient in Eq. (75a) is consistent with the general result in Eq. (68). We see that Debye filtering of a Markovian

trajectory produces non-Markovianity in the form of a single-exponential memory kernel with a memory time  $\tau_f$  that is strictly shorter than the Debye filter decay time  $\lambda$ . The friction coefficient  $\gamma_f$  of the filtered trajectory can be larger or smaller than the friction coefficient  $\gamma$  of the unfiltered Markovian trajectory, only for an unconfined trajectory with  $K = 0$  do we know for sure that the friction coefficient  $\gamma_f$  of the filtered trajectory goes down compared to the friction coefficient  $\gamma$  of the unfiltered Markovian trajectory,

#### IV. DISCUSSION

We have shown that the dynamics of convolution filtered observables obey the Liouville equation just as regular observables do. Based on this finding we derived the GLE for filtered observables by exact projection in phase space, which has the same structure as the GLE for regular observables. We derived explicit transformation formulas that allow us to calculate the parameters of the filtered GLE from parameters of the unfiltered GLE and vice versa.

There are two major applications of our filter-projection approach: Low-pass filtering eliminates fast data components and thereby yields a temporally coarse-grained model. Our filter-projection approach not only shows that the GLE is the exact equation of motion for such temporally coarse-grained variable, it also provides all the parameters of the filtered GLE.

Conversely, the elimination of slow or periodic data components by high-pass or band-stop filtering is important in many practical situations. The standard approach towards such systems would be to use non-equilibrium statistical mechanics methods, for example based on a time-dependent Hamiltonian. The concept of a time-dependent Hamiltonian derives from splitting the autonomous time-independent Hamiltonian, which encompasses the system components that cause the slow transient or seasonal dynamics, into the system of interest and its slowly evolving environment. The coupling between the system of interest and the environment then leads to time-dependent terms in the system Hamiltonian. Recently, time-dependent projection techniques have been used to derive non-equilibrium GLEs for systems that are described by time-dependent Liouville operators [55, 57]. Even more recently it was shown that systems described by time-dependent Hamiltonians can also be treated by time-independent projection techniques [45]. In the present filter-projection approach there is no need to introduce a time-dependent Hamiltonian or Liouville operator, rather, the Hamiltonian can be considered time-independent and large enough so that it includes the system components causing the slow and transient dynamics. The slow and transient data components are then removed by filtering. In that sense, our filter-projection approach constitutes an alternative to the usual non-equilibrium approach to systems that

exhibit slow transient effects, such as active systems, weather or financial data.

In this work we assume that the trajectory of a given observable comes from simulations or experiments and obeys classical autonomous Hamiltonian dynamics, the interesting case of quantum dynamics has not been treated. Also, the question of the existence of an optimal observable for characterizing the system dynamics is important but was not considered. Finally, we remark that although the effect of discretization of continuous data can not be described as a convolution filter, the effect of discretization is expected to be reduced by prior low-pass filtering.

## ACKNOWLEDGMENTS

We acknowledge support by Deutsche Forschungsgemeinschaft Grant CRC 1114 "Scaling Cascades in Complex System", Project 235221301, Project B03 and by the ERC Advanced Grant 835117 NoMaMemo and by the Infosys Foundation. We gratefully acknowledge computing time on the HPC clusters at the physics department and ZEDAT, FU Berlin.

### Appendix A: Derivation of the GLE for filtered observable

We begin with the derivation of a few important properties of the Mori projection operator in Eq. (31), which we split into three parts according to

$$\mathcal{P}A(\omega, t) = \mathcal{P}_1A(\omega, t) + \mathcal{P}_2A(\omega, t) + \mathcal{P}_3A(\omega, t) \quad (\text{A1})$$

with

$$\mathcal{P}_1A(\omega, t) = \langle A(\omega, t) \rangle, \quad (\text{A2})$$

$$\mathcal{P}_2A(\omega, t) = \frac{\langle A(\omega, t) \mathcal{L} B_f(\omega, t_P) \rangle}{\langle (\mathcal{L} B_f(\omega, t_P))^2 \rangle} \mathcal{L} B_f(\omega, t_P), \quad (\text{A3})$$

$$\mathcal{P}_3A(\omega, t) = \frac{\langle A(\omega, t)(B_f(\omega, t_P) - \langle B_f \rangle) \rangle}{\langle (B_f(\omega, t_P) - \langle B_f \rangle)^2 \rangle} (B_f(\omega, t_P) - \langle B_f \rangle). \quad (\text{A4})$$

The linearity of the Mori projection, i.e., the fact that for two arbitrary observables  $A(\omega, t)$  and  $C(\omega, t')$  the property  $\mathcal{P}(c_1A(\omega, t) + c_2C(\omega, t')) = c_1\mathcal{P}A(\omega, t) + c_2\mathcal{P}C(\omega, t')$  holds, is self-evident,  $\mathcal{Q}$  thereby also follows to be linear. The idempotency of  $\mathcal{P}$ , i.e., the fact that  $\mathcal{P}^2 = \mathcal{P}$ , is not so self-evident and the proof will be split into three parts. First,

$$\begin{aligned} \mathcal{P}\mathcal{P}_1A(\omega, t) &= \langle A(\omega, t) \rangle \left[ 1 + \frac{\langle \mathcal{L} B_f(\omega, t_P) \rangle}{\langle (\mathcal{L} B_f(\omega, t_P))^2 \rangle} \mathcal{L} B_f(\omega, t_P) + \frac{\langle B_f(\omega, t_P) - \langle B_f \rangle \rangle}{\langle (B_f(\omega, t_P) - \langle B_f \rangle)^2 \rangle} (B_f(\omega, t_P) - \langle B_f \rangle) \right] \\ &= \mathcal{P}_1A(\omega, t). \end{aligned} \quad (\text{A5})$$

We used that  $\langle \langle A(\omega, t) \rangle \rangle = \langle A(\omega, t) \rangle$ , which holds since the probability distribution  $\rho_P(\omega)$  in Eq. (32) is normalized. For the second term we used the anti-self-adjointness of the Liouville operator  $\mathcal{L}$  and the stationarity of the projection distribution, i.e.  $\mathcal{L}\rho_P(\omega) = 0$ . Second,

$$\begin{aligned} \mathcal{P}\mathcal{P}_2A(\omega, t) &= \frac{\langle A(\omega, t) \mathcal{L} B_f(\omega, t_P) \rangle}{\langle (\mathcal{L} B_f(\omega, t_P))^2 \rangle} \\ &\times \left[ \langle \mathcal{L} B_f(\omega, t_P) \rangle + \frac{\langle (\mathcal{L} B_f(\omega, t_P))^2 \rangle}{\langle (\mathcal{L} B_f(\omega, t_P))^2 \rangle} \mathcal{L} B_f(\omega, t_P) + \frac{\langle (B_f(\omega, t_P) - \langle B_f \rangle) \mathcal{L} B_f(\omega, t_P) \rangle}{\langle (B_f(\omega, t_P) - \langle B_f \rangle)^2 \rangle} (B_f(\omega, t_P) - \langle B_f \rangle) \right] \\ &= \mathcal{P}_2B(\omega, t), \end{aligned} \quad (\text{A6})$$

where again we used the anti-self-adjointness of  $\mathcal{L}$  and the stationarity of  $\rho_P(\omega)$ . Third,

$$\begin{aligned} \mathcal{P}\mathcal{P}_3A(\omega, t) &= \frac{\langle A(\omega, t)(B_f(\omega, t_P) - \langle B_f \rangle) \rangle}{\langle (B_f(\omega, t_P) - \langle B_f \rangle)^2 \rangle} \\ &\times \left[ \langle B_f(\omega, t_P) - \langle B_f \rangle \rangle + \frac{\langle (B_f(\omega, t_P) - \langle B_f \rangle) \mathcal{L} B_f(\omega, t_P) \rangle}{\langle (\mathcal{L} B_f(\omega, t_P))^2 \rangle} \mathcal{L} B_f(\omega, t_P) + \frac{\langle (B_f(\omega, t_P) - \langle B_f \rangle)^2 \rangle}{\langle (B_f(\omega, t_P) - \langle B_f \rangle)^2 \rangle} (B_f(\omega, t_P) - \langle B_f \rangle) \right] \\ &= \mathcal{P}_3B(\omega, t). \end{aligned} \quad (\text{A7})$$

Adding Eqs. (A5), (A6), (A7) we see that  $\mathcal{P}^2 = \mathcal{P}(\mathcal{P}_1 + \mathcal{P}_2 + \mathcal{P}_3) = \mathcal{P}_1 + \mathcal{P}_2 + \mathcal{P}_3 = \mathcal{P}$  and thus  $\mathcal{P}$  is idempotent. From the idempotency of  $\mathcal{P}$  the idempotency of  $\mathcal{Q}$  also follows, this can be easily seen from

$$\mathcal{Q}^2 A(\omega, t) = (1 - \mathcal{P})^2 A(\omega, t) = (1 - 2\mathcal{P} + \mathcal{P}^2) A(\omega, t) = (1 - \mathcal{P}) A(\omega, t) = \mathcal{Q} A(\omega, t). \quad (\text{A8})$$

The self-adjointness of  $\mathcal{P}$ , Eq. (33), is straightforwardly proven by writing

$$\langle C(\omega, t) \mathcal{P} A(\omega, t') \rangle = \quad (\text{A9})$$

$$\langle C(\omega, t) \rangle \langle A(\omega, t') \rangle + \langle C(\omega, t) \mathcal{L} B_f(\omega, t_P) \rangle \frac{\langle A(\omega, t') \mathcal{L} B_f(\omega, t_P) \rangle}{\langle (\mathcal{L} B_f(\omega, t_P))^2 \rangle} + \langle C(\omega, t) (B_f(\omega, t_P) - \langle B_f \rangle) \rangle \frac{\langle A(\omega, t') (B_f(\omega, t_P) - \langle B_f \rangle) \rangle}{\langle (B_f(\omega, t_P) - \langle B_f \rangle)^2 \rangle} \quad (\text{A10})$$

$$= \langle A(\omega, t') \mathcal{P} C(\omega, t) \rangle. \quad (\text{A11})$$

By using  $\mathcal{Q} = 1 - \mathcal{P}$  we see straightforwardly that  $\mathcal{Q}$  is also self-adjoint.

Using similar arguments as above, one can show that  $\mathcal{P}c = c$ ,  $\mathcal{P}(B_f(\omega, t_P) - \langle B_f \rangle) = B_f(\omega, t_P) - \langle B_f \rangle$ ,  $\mathcal{P} \mathcal{L} B_f(\omega, t_P) = \mathcal{L} B_f(\omega, t_P)$ , from which follows that also  $\mathcal{P} B_f(\omega, t_P) = B_f(\omega, t_P)$ . From these relations we can directly conclude that  $\mathcal{Q}c = 0$ ,  $\mathcal{Q}(B_f(\omega, t_P) - \langle B_f \rangle) = 0$ ,  $\mathcal{Q} \mathcal{L} B_f(\omega, t_P) = 0$ , and also  $\mathcal{Q} B_f(\omega, t_P) = 0$ . From the idempotency of  $\mathcal{P}$  or  $\mathcal{Q}$  it follows that  $\mathcal{P} \mathcal{Q} = \mathcal{P}(1 - \mathcal{P}) = \mathcal{P} - \mathcal{P}^2 = 0$  and, similarly,  $\mathcal{Q} \mathcal{P} = 0$ , thus, the operators  $\mathcal{P}$  and  $\mathcal{Q}$  are orthogonal to each other.

We now derive the GLE and consider the first term on the right-hand side in Eq. (29), which, apart from the propagator in front, splits into three terms

$$\mathcal{P} \mathcal{L}^2 B_f(\omega, t_P) = (\mathcal{P}_1 + \mathcal{P}_2 + \mathcal{P}_3) \mathcal{L}^2 B_f(\omega, t_P). \quad (\text{A12})$$

The first term is given by

$$\mathcal{P}_1 \mathcal{L}^2 B_f(\omega, t_P) = \langle \mathcal{L}^2 B_f(\omega, t_P) \rangle = 0, \quad (\text{A13})$$

where we used the anti-self-adjointness of  $\mathcal{L}$  and the stationarity of  $\rho_P(\omega)$ . The second term reads

$$\mathcal{P}_2 \mathcal{L}^2 B_f(\omega, t_P) = \frac{\langle (\mathcal{L} B_f(\omega, t_P)) \mathcal{L}^2 B_f(\omega, t_P) \rangle}{\langle (\mathcal{L} B_f(\omega, t_P))^2 \rangle} \mathcal{L} B_f(\omega, t_P) = 0. \quad (\text{A14})$$

The third term reads

$$\begin{aligned} \mathcal{P}_3 \mathcal{L}^2 B_f(\omega, t_P) &= \frac{\langle (B_f(\omega, t_P) - \langle B_f \rangle) \mathcal{L}^2 B_f(\omega, t_P) \rangle}{\langle (B_f(\omega, t_P) - \langle B_f \rangle)^2 \rangle} (B_f(\omega, t_P) - \langle B_f \rangle) \\ &= - \frac{\langle \mathcal{L} B_f(\omega, t_P) \rangle}{\langle (B_f(\omega, t_P) - \langle B_f \rangle)^2 \rangle} (B_f(\omega, t_P) - \langle B_f \rangle). \end{aligned} \quad (\text{A15})$$

Combining the results in Eqs. (A12), (A13), (A14), (A15), the first term in Eq. (29) reads

$$\begin{aligned} e^{(t-t_P)\mathcal{L}} \mathcal{P} \mathcal{L}^2 B_f(\omega, t_P) &= -K_f e^{(t-t_P)\mathcal{L}} (B_f(\omega, t_P) - \langle B_f \rangle) \\ &= -K_f (B_f(\omega, t) - \langle B_f \rangle) \end{aligned} \quad (\text{A16})$$

where  $K_f$  is defined in Eqs. (35).

We now consider the last term on the right-hand side in Eq. (29), which reads, without the time integral and the propagator in front,

$$\mathcal{P} \mathcal{L} F(\omega, s + t_P) = (\mathcal{P}_1 + \mathcal{P}_2 + \mathcal{P}_3) \mathcal{L} F(\omega, s + t_P). \quad (\text{A17})$$

The first term is given by

$$\mathcal{P}_1 \mathcal{L} F(\omega, s + t_P) = \langle \mathcal{L} F(\omega, s + t_P) \rangle = 0, \quad (\text{A18})$$

where we used the anti-self-adjointness of  $\mathcal{L}$  and the stationarity of  $\rho_P(\omega)$ . The second term reads

$$\begin{aligned} \mathcal{P}_2 \mathcal{L} F(\omega, s + t_P) &= \frac{\langle (\mathcal{L} F(\omega, s + t_P)) \mathcal{L} B_f(\omega, t_P) \rangle}{\langle (\mathcal{L} B_f(\omega, t_P))^2 \rangle} \mathcal{L} B_f(\omega, t_P) = - \frac{\langle F(\omega, s + t_P) \mathcal{L}^2 B_f(\omega, t_P) \rangle}{\langle (\mathcal{L} B_f(\omega, t_P))^2 \rangle} \mathcal{L} B_f(\omega, t_P) \\ &= - \frac{\langle (\mathcal{Q} F(\omega, s + t_P)) \mathcal{L}^2 B_f(\omega, t_P) \rangle}{\langle (\mathcal{L} B_f(\omega, t_P))^2 \rangle} \mathcal{L} B_f(\omega, t_P) = - \frac{\langle F(\omega, s + t_P) \mathcal{Q} \mathcal{L}^2 B_f(\omega, t_P) \rangle}{\langle (\mathcal{L} B_f(\omega, t_P))^2 \rangle} \mathcal{L} B_f(\omega, t_P) \\ &= - \frac{\langle F(\omega, s + t_P) F(\omega, t_P) \rangle}{\langle (\mathcal{L} B_f(\omega, t_P))^2 \rangle} \mathcal{L} B_f(\omega, t_P) = - \frac{\langle F(\omega, s) F(\omega, 0) \rangle}{\langle (\mathcal{L} B_f(\omega, t_P))^2 \rangle} \mathcal{L} B_f(\omega, t_P), \end{aligned} \quad (\text{A19})$$

where we used the anti-self-adjointness of  $\mathcal{L}$  and the stationarity of  $\rho_P(\omega)$ , the idempotency and self-adjointness of  $\mathcal{Q}$  as well as the definition of the complementary force in Eq. (30). The third term reads

$$\begin{aligned}
\mathcal{P}_3 \mathcal{L} F(\omega, s + t_P) &= \frac{\langle (\mathcal{L} F(\omega, s + t_P))(B_f(\omega, t_P) - \langle B_f \rangle) \rangle}{\langle (B_f(\omega, t_P) - \langle B_f \rangle)^2 \rangle} (B_f(\omega, t_P) - \langle B_f \rangle) \\
&= - \frac{\langle F(\omega, s + t_P) \mathcal{L} B_f(\omega, t_P) \rangle}{\langle (B_f(\omega, t_P) - \langle B_f \rangle)^2 \rangle} (B_f(\omega, t_P) - \langle B_f \rangle) \\
&= - \frac{\langle (\mathcal{Q} F(\omega, s + t_P)) \mathcal{L} B_f(\omega, t_P) \rangle}{\langle (B_f(\omega, t_P) - \langle B_f \rangle)^2 \rangle} (B_f(\omega, t_P) - \langle B_f \rangle) \\
&= - \frac{\langle F(\omega, s + t_P) \mathcal{Q} \mathcal{L} B_f(\omega, t_P) \rangle}{\langle (B_f(\omega, t_P) - \langle B_f \rangle)^2 \rangle} (B_f(\omega, t_P) - \langle B_f \rangle) = 0,
\end{aligned} \tag{A20}$$

where we used the anti-self-adjointness of  $\mathcal{L}$  and the stationarity of  $\rho_P(\omega)$ , the idempotency and self-adjointness of  $\mathcal{Q}$ , the definition of the complementary force in Eq. (30) as well as the fact that  $\mathcal{Q} \mathcal{L} B_f(\omega, t_P) = 0$ . Combining the results in Eqs. (A17), (A18), (A19), (A20), the integrand in the last term on the right-hand side in Eq. (29) reads

$$\begin{aligned}
e^{(t-t_P-s)\mathcal{L}} \mathcal{P} \mathcal{L} F(\omega, s + t_P) &= -\Gamma_f(s) e^{(t-t_P-s)\mathcal{L}} \mathcal{L} B_f(\omega, t_P) \\
&= -\Gamma_f(s) \mathcal{L} B_f(\omega, t - s)
\end{aligned} \tag{A21}$$

where  $\Gamma_f(s)$  is defined in Eqs. (36). Inserting the results in Eqs. (A16) and (A21) into the general GLE in Eq. (29) we obtain the explicit Mori GLE in Eq. (34).

## Appendix B: Derivation of the Debye-filtered mean-squared position and mean-squared velocity

Here we derive Eqs. (66a) and (66b) by residual calculus. Combining Eqs. (61a) and (70) we obtain

$$\langle x_f^2 \rangle = \int \frac{d\nu}{2\pi} \tilde{C}_{xx}^f(\nu) = \int \frac{d\nu}{2\pi} \nu^2 \tilde{f}(\nu) \tilde{f}(-\nu) \tilde{C}_{xx}(\nu) = \int \frac{d\nu}{2\pi} \tilde{f}(\nu) \tilde{f}(-\nu) \frac{\langle \dot{x}^2 \rangle}{i\nu} [\tilde{\chi}(-\nu) - \tilde{\chi}(\nu)]. \tag{B1}$$

Inserting the Fourier transform of the Debye filter from Eq. (65) we obtain

$$\langle x_f^2 \rangle = \langle \dot{x}^2 \rangle \int \frac{d\nu}{2\pi} \frac{1}{i\nu(1 + \lambda^2 \nu^2)} [\tilde{\chi}(-\nu) - \tilde{\chi}(\nu)]. \tag{B2}$$

The response function of the unfiltered system  $\tilde{\chi}(\nu)$  is given in Eq. (69). Since the time-domain response function  $\chi(t)$  is a single-sided decaying function,  $\tilde{\chi}(\nu)$  has no poles in the lower complex plane while  $\tilde{\chi}(-\nu)$  has no poles in the upper complex plane. We thus close the integration contour in Eq. (B2) of the integrand proportional to  $\tilde{\chi}(\nu)$  in the lower complex plane and of the integrand proportional to  $\tilde{\chi}(-\nu)$  in the lower complex plane. The residuals of the three poles at  $\nu = 0$ ,  $\nu = \pm i/\lambda$  give rise to the final result

$$\langle x_f^2 \rangle = \langle \dot{x}^2 \rangle \left[ \frac{1}{K} - \frac{\lambda^2}{1 + K\lambda^2 + \lambda \tilde{\Gamma}(-i/\lambda)} \right]. \tag{B3}$$

Similarly, by combining Eqs. (61b), (56) and (70) we obtain

$$\langle \dot{x}_f^2 \rangle = \langle \dot{x}^2 \rangle \int \frac{d\nu}{2\pi} \frac{\nu^2}{i\nu(1 + \lambda^2 \nu^2)} [\tilde{\chi}(-\nu) - \tilde{\chi}(\nu)], \tag{B4}$$

which by residual calculus yields the final result

$$\langle \dot{x}_f^2 \rangle = \frac{\langle \dot{x}^2 \rangle}{1 + K\lambda^2 + \lambda \tilde{\Gamma}(-i/\lambda)} \tag{B5}$$

in Eq. (66b). Eq. (66a) follows from Eq. (B3) by dividing by  $K = \langle \dot{x}^2 \rangle / \langle x^2 \rangle$ .

### Appendix C: Derivation of Debye-filtered memory kernel for Markovian unfiltered system

We start the derivation of Eqs. (73), (75a) and (75b) by slightly rewriting Eq. (71) as

$$\begin{aligned}
 \tilde{\chi}_f(-\nu) - \tilde{\chi}_f(\nu) &= \frac{1}{K_f - \nu^2 - \nu \tilde{\Gamma}_f(-\nu)} - \frac{1}{K_f - \nu^2 + \nu \tilde{\Gamma}_f(\nu)} \\
 &= \frac{\langle \dot{x}^2 \rangle}{\langle \dot{x}_f^2 \rangle} \left[ \frac{1}{K - \nu^2 - \nu \gamma} - \frac{1}{K - \nu^2 + \nu \gamma} \right] \frac{1}{1 + \lambda^2 \nu^2} \\
 &= \frac{\langle \dot{x}^2 \rangle}{\langle \dot{x}_f^2 \rangle} \left[ \frac{1}{\nu^2 - \nu \gamma - K} - \frac{1}{\nu^2 + \nu \gamma - K} \right] \frac{\lambda^{-2}}{\nu^2 + \lambda^{-2}} \\
 &= \frac{\langle \dot{x}^2 \rangle}{\langle \dot{x}_f^2 \rangle} \left[ \frac{1}{(\nu - \nu_1)(\nu - \nu_2)} - \frac{1}{(\nu - \nu_3)(\nu - \nu_4)} \right] \frac{\lambda^{-2}}{(\nu - \nu_5)(\nu - \nu_6)}. \tag{C1}
 \end{aligned}$$

As already mentioned in the main text, while on the left-hand side of Eq. (C1) the expressions  $\tilde{\chi}_f(-\nu)$  and  $\tilde{\chi}_f(\nu)$  correspond to separate anticausal and causal terms, the filtering mixes the six anticausal and causal poles on the right-hand side of Eq. (C1). The six poles are given by

$$\begin{aligned}
 \nu_{1,2} &= \frac{\nu \gamma}{2} \pm \sqrt{K - \gamma^2/4}, \\
 \nu_{3,4} &= -\frac{\nu \gamma}{2} \pm \sqrt{K - \gamma^2/4}, \\
 \nu_{5,6} &= \pm i \lambda^{-1}. \tag{C2}
 \end{aligned}$$

The poles  $\nu_{1,2}$  are located in the upper complex plane and are thus causal, the poles  $\nu_{3,4}$  are located in the lower complex plane and are thus anticausal, the pole  $\nu_5 = i \lambda^{-1}$  is causal and the pole  $\nu_6 = -i \lambda^{-1}$  is anticausal. By basic algebraic operations the right-hand side of Eq. (C1) can be separated into a causal and an anticausal part. The causal part turns out to be given by

$$\tilde{\chi}_f(\nu) = \frac{1}{K_f - \nu^2 + \nu \tilde{\Gamma}_f(\nu)} = \frac{\nu \gamma + i \lambda^{-1} - \nu}{(\nu - \nu_1)(\nu - \nu_2)(\nu - \nu_5)}. \tag{C3}$$

Solving for  $\tilde{\Gamma}_f(\nu)$  one obtains the result in Eq. (73) with the friction coefficient  $\gamma_f$  given by Eq. (75a) and the memory time  $\tau_f$  given by Eq. (75b).

- 
- |  |  |
|--|--|
| <p>[1] M. Levitt and A. Warshel, Computer simulation of protein folding, <i>Nature</i> <b>253</b>, 694 (1975).</p> <p>[2] S. Kmiecik, D. Gront, M. Kolinski, L. Wieteska, A. E. Dawid, and A. Kolinski, Coarse-Grained Protein Models and Their Applications, <i>Chem. Rev.</i> <b>116</b>, 7898 (2016).</p> <p>[3] P. S. Walmod, R. Hartmann-Petersen, S. Prag, E. L. Lepekhin, C. Röpke, V. Berezin, and E. Bock, Cell-cycle-dependent regulation of cell motility and determination of the role of Rac1, <i>Experimental Cell Research</i> <b>295</b>, 407 (2004).</p> <p>[4] C. L. E. Franzke, T. J. O’Kane, J. Berner, P. D. Williams, and V. Lucarini, <i>Stochastic Climate Theory and Modeling</i>, Wiley Interdisciplinary Reviews: Climate Change <b>6</b>, 63 (2015).</p> <p>[5] J. Gunawardena, Time-scale separation – Michaelis and Menten’s old idea, still bearing fruit, <i>FEBS Journal</i> <b>281</b>, 473 (2014).</p> <p>[6] L. Tepper, B. A. Dalton, and R. R. Netz, Accurate</p> | <p>Memory Kernel Extraction from Discretized Time-Series Data, <i>Journal of Chemical Theory and Computation</i> <b>20</b>, 3061 (2024).</p> <p>[7] H. Changbon and D. Thirumalai, Capturing the essence of folding and functions of biomolecules using coarse-grained models, <i>Nature Communications</i> <b>2</b>, 487 (2011).</p> <p>[8] N. A. Denesyuk and D. Thirumalai, Coarse-graining DNA for simulations of DNA nanotechnology, <i>Phys. Chem. Chem. Phys.</i> <b>15</b>, 20395 (2013).</p> <p>[9] J. P. K. e. a. Doye, Time-scale separation – Michaelis and Menten’s old idea, still bearing fruit, <i>FEBS Journal</i> <b>281</b>, 473 (2014).</p> <p>[10] D. A. Potoyan, A. Savelyev, and G. A. Papoian, Recent successes in coarse-grained modeling of DNA, <i>WIREs Comput Mol Sci</i> <b>3</b>, 69 (2013).</p> <p>[11] P. C. T. e. a. Souza, Martini 3: a general purpose force field for coarse-grained molecular dynamics, <i>Nature Methods</i> <b>18</b>, 382 (2021).</p> |
|--|--|

- [12] J. Wang, S. Olsson, C. Wehmeyer, A. Perez, N. E. Charon, G. de Fabritiis, F. Noe, and C. Clementi, Machine Learning of Coarse-Grained Molecular Dynamics Force Fields, *ACS Cent. Sci.* **5**, 755 (2019).
- [13] C. Ayaz, L. Tepper, F. N. Brünig, J. Kappler, J. O. Daldrop, and R. R. Netz, Non-Markovian modeling of protein folding, *Proceedings of the National Academy of Sciences* **118**, 10.1073/pnas.2023856118 (2021), publisher: National Academy of Sciences Section: Physical Sciences.
- [14] B. A. Dalton, C. Ayaz, H. Kiefer, A. Klimek, L. Tepper, and R. R. Netz, Fast protein folding is governed by memory-dependent friction, *Proceedings of the National Academy of Sciences* **120**, e2220068120 (2023).
- [15] D. T. Schmitt and M. Schulz, Analyzing Memory Effects of Complex Systems from Time Series, *Physical Review E* **73**, 056204 (2006).
- [16] I. Prigogine and P. Mazur, Sur l'extension de la thermodynamique aux phenomenes irreversibles lies aux degres de liberte internes, *Physica* **XIX**, 241 (1953).
- [17] J. L. Lebowitz, Stationary nonequilibrium Gibbsian ensembles, *Phys. Rev.* **114**, 1192 (1959).
- [18] R. Zwanzig, Ensemble method in the theory of irreversibility, *The Journal of Chemical Physics* **33**, 1338 (1960).
- [19] S. R. de Groot and P. Mazur, *Non-Equilibrium Thermodynamics* (North-Holland Pub. Co., Amsterdam, 1962).
- [20] B. Schmittmann and R. K. P. Zia, Driven diffusive systems. an introduction and recent developments, *Phys. Rep.* **301**, 45 (1998).
- [21] B. Derrida, J. L. Lebowitz, and E. R. Speer, Free energy functional for nonequilibrium systems: An exactly solvable case, *Phys. Rev. Lett.* **87**, 150601 (2001).
- [22] P. Ilg and J. L. Barrat, From single-particle to collective effective temperatures in an active fluid of self-propelled particles, *Europhys. Lett.* **111**, 26001 (2007).
- [23] E. Fodor, C. Nardini, M. E. Cates, J. Tailleur, P. Visco, and F. van Wijland, How far from equilibrium is active matter?, *Phys. Rev. Lett.* **117**, 038103 (2016).
- [24] C. Jarzynski, Hamiltonian derivation of a detailed fluctuation theorem, *Journal of Statistical Physics* **98**, 77 (2000).
- [25] T. Harada and S. I. Sasa, Equality connecting energy dissipation with a violation of the fluctuation-response relation, *Phys. Rev. Lett.* **95**, 130602 (2005).
- [26] U. Seifert, Entropy production along a stochastic trajectory and an integral fluctuation theorem, *Phys. Rev. Lett.* **95**, 040602 (2005).
- [27] J. Prost, J.-F. Joanny, and J. M. R. Parrondo, Generalized fluctuation-dissipation theorem for steady-state systems, *Phys. Rev. Lett.* **103**, 090601 (2009).
- [28] M. Baiesi, C. Maes, and B. Wynants, Fluctuations and response of nonequilibrium states, *Phys. Rev. Lett.* **103**, 010602 (2009).
- [29] U. Seifert and T. Speck, Fluctuation-dissipation theorem in nonequilibrium steady states, *Europhys. Lett.* **89**, 10007 (2010).
- [30] R. R. Netz, Approach to equilibrium and nonequilibrium stationary distributions of interacting many-particle systems that are coupled to different heat baths, *Phys. Rev. E* **101**, 022120 (2020).
- [31] H. Mori, Transport, Collective Motion, and Brownian Motion, *Progress of Theoretical Physics* **33**, 423 (1965).
- [32] R. Zwanzig, Memory Effects in Irreversible Thermodynamics, *Physical Review* **124**, 983 (1961).
- [33] J. E. Straub, M. Borkovec, and B. J. Berne, Calculation of dynamic friction on intramolecular degrees of freedom, *The Journal of Physical Chemistry* **91**, 4995 (1987).
- [34] J. O. Daldrop, J. Kappler, F. N. Brünig, and R. R. Netz, Butane dihedral angle dynamics in water is dominated by internal friction, *Proceedings of the National Academy of Sciences* **115**, 5169 (2018), publisher: National Academy of Sciences Section: Biological Sciences.
- [35] B. Kowalik, J. O. Daldrop, J. Kappler, J. C. F. Schulz, A. Schlaich, and R. R. Netz, Memory-kernel extraction for different molecular solutes in solvents of varying viscosity in confinement, *Physical Review E* **100**, 012126 (2019).
- [36] F. Grogan, H. Lei, X. Li, and N. A. Baker, Data-Driven Molecular Modeling with the Generalized Langevin Equation, *Journal of Computational Physics* **418**, 109633 (2020).
- [37] R. Satija and D. E. Makarov, Generalized Langevin Equation as a Model for Barrier Crossing Dynamics in Biomolecular Folding, *The Journal of Physical Chemistry B* **123**, 802 (2019), publisher: American Chemical Society.
- [38] F. N. Brünig, O. Geburtig, A. von Canal, J. Kappler, and R. R. Netz, Time-Dependent Friction Effects on Vibrational Infrared Frequencies and Line Shapes of Liquid Water, *The Journal of Physical Chemistry B* **126**, 1579 (2022).
- [39] F. N. Brünig, J. O. Daldrop, and R. R. Netz, Pair-Reaction Dynamics in Water: Competition of Memory, Potential Shape, and Inertial Effects, *The Journal of Physical Chemistry B* **126**, 10295 (2022).
- [40] B. A. Dalton, H. Kiefer, and R. R. Netz, The Role of Memory-Dependent Friction and Solvent Viscosity in Isomerization Kinetics in Viscogenic Media, *Nature Communications* **15**, 3761 (2024).
- [41] B. G. Mitterwallner, C. Schreiber, J. O. Daldrop, J. O. Rädler, and R. R. Netz, Non-Markovian data-driven modeling of single-cell motility, *Physical Review E* **101**, 032408 (2020).
- [42] F. Hassanibesheli, N. Boers, and J. Kurths, Reconstructing Complex System Dynamics from Time Series: A Method Comparison, *New Journal of Physics* **22**, 073053 (2020).
- [43] A. Klimek, D. Mondal, S. Block, P. Sharma, and R. R. Netz, Data-driven classification of individual cells by their non-Markovian motion, *Biophysical Journal* **123**, 1 (2024).
- [44] R. Zwanzig, *Nonequilibrium statistical mechanics* (Oxford UnivPress, Oxford [u.a.], 2001).
- [45] R. R. Netz, Derivation of the nonequilibrium generalized langevin equation from a time-dependent many-body hamiltonian, *Phys. Rev. E* **110**, 014123 (2024).
- [46] F. J. Dyson, *The Radiation Theories of Tomonaga, Schwinger, and Feynman*, *Physical Review* **75**, 486 (1949), publisher: American Physical Society.
- [47] R. P. Feynman, An Operator Calculus Having Applications in Quantum Electrodynamics, *Physical Review* **84**, 108 (1951), publisher: American Physical Society.
- [48] D. J. Evans, *Statistical mechanics of nonequilibrium liquids / Denis J. Evans*, second edition. ed. (University Press, Cambridge, 2008) book Title: *Statistical mechanics of nonequilibrium liquids*.

- [49] C. Ayaz, L. Scalfi, B. A. Dalton, and R. R. Netz, Generalized langevin equation with a nonlinear potential of mean force and nonlinear memory friction from a hybrid projection scheme, *Physical Review E* **105**, 054138 (2022).
- [50] H. Vroylandt, On the derivation of the generalized langevin equation and the fluctuation-dissipation theorem, *Europhys. Lett.* **140**, 62003 (2022).
- [51] C. Ayaz, L. Tepper, and R. R. Netz, Markovian embedding of generalized langevin equations with a nonlinear friction kernel and configuration-dependent mass, *Turk. J. Phys.* **46**, 194 (2022).
- [52] A. Carof, R. Vuilleumier, and B. Rotenberg, Two algorithms to compute projected correlation functions in molecular dynamics simulations, *The Journal of Chemical Physics* **140**, 124103 (2014), publisher: American Institute of Physics.
- [53] D. Lesnicki, R. Vuilleumier, A. Carof, and B. Rotenberg, Molecular Hydrodynamics from Memory Kernels, *Physical Review Letters* **116**, 147804 (2016), publisher: American Physical Society.
- [54] H. Vroylandt, L. Goudenège, P. Monmarché, F. Pietrucci, and B. Rotenberg, Likelihood-based non-markovian models from molecular dynamics, *Proceedings of the National Academy of Sciences* **119**, e2117586119 (2022).
- [55] H. Meyer, T. Voigtmann, and T. Schilling, On the non-stationary generalized Langevin equation, *The Journal of Chemical Physics* **147**, 214110 (2017), publisher: American Institute of Physics.
- [56] H. Meyer, P. Pelagejcev, and T. Schilling, Non-Markovian out-of-equilibrium dynamics: A general numerical procedure to construct time-dependent memory kernels for coarse-grained observables, *EPL (Europhysics Letters)* **128**, 40001 (2020), publisher: IOP Publishing.
- [57] M. te Vrugt and R. Wittkowski, Mori-zwanzig projection operator formalism for far-from-equilibrium systems with time-dependent hamiltonians, *Physical Review E* **99**, 062118 (2019).